arXiv:cond-mat/0409118v1 [cond-mat.str-el] 6 Sep 2004

Antiferromagnetic, Neutral, and Superconducting Band in La_2CuO_4

Ekkehard Krüger
Max-Planck-Institut für Metallforschung, D-70506 Stuttgart, Germany
(Dated: April 14, 2024)

The symmetry of the Bloch functions in the conduction band of tetragonal and orthorhombic La_2CuO_4 is examined for the existence of symmetry-adapted and optimally localizable (usual or spin-dependent) Wannier functions. It turns out that such Wannier functions do not exist in the tetragonal phase. In the orthorhombic phase, on the other hand, the Bloch functions can be unitarily transformed in three different ways into optimally localizable Wannier functions: they can be chosen to be adapted to each of the three phases observed in the pure or doped material, that is, to the antiferromagnetic phase, to the superconducting phase or to the phase evincing neither magnetism nor superconductivity. This group-theoretical result is proposed to be interpreted within a nonadiabatic extension of the Heisenberg model. Within this model, atomiclike states represented by these Wannier functions are responsible for the stability of each of the three phases. However, all the three atomiclike states cannot exist in the tetragonal phase, but are stabilized by the orthorhombic distortion of the crystal. A simple model is proposed which might explain the physical properties of $La_{2-x}Sr_xCuO_4$ as a function of the Sr concentration x.

Keywords: superconductivity, magnetism, Heisenberg model, group theory

1. INTRODUCTION

1.1. $La_{2-x}Sr_xCuO_4$

The physical properties of pure and doped $La_{2-x}Sr_xCuO_4$ have been studied in a broad range of Sr concentrations x [1, 2]. Pure La_2CuO_4 is antiferromagnetic below about 300 K, but this magnetic long-range order disappears at a Sr concentration of $x \approx 0.015$. Between $x \approx 0.015$ and $x \approx 0.05$ the samples evince neither an antiferromagnetic or a superconducting state. This border region has features characteristic of spin-glass systems [3]. Finally, above $x \approx 0.05$ the material becomes a high-T_c superconductor.

Furthermore, La_2CuO_4 undergoes a very interesting structural phase transition at about 520 K from a high-temperature tetragonal phase to a low-temperature orthorhombic phase [1]. The tetragonal structure with the space group $I4/mmm$ is depicted in Fig. 1. The major change in the structure in the tetragonal to orthorhombic transition involves a "buckling of the copper-oxygen planes" [2]: in the orthorhombic phase with the space group $Cmca$ the oxygen atoms are slightly shifted from their tetragonal positions in such a way that the translation $\vec{t}_3$ in Fig. 1 is doubled [1, 2], see Fig. 2. The orthorhombic distortion is so small that the orthorhombic and tetragonal structures are not distinguishable on the scale of the figures [2].

The buckling of the copper-oxygen planes has been established also in doped $La_{2-x}Sr_xCuO_4$ for a broad range of Sr concentrations x. At zero temperature, is exists up to $x \approx 0.2$ and disappears for higher Sr concentrations [1].

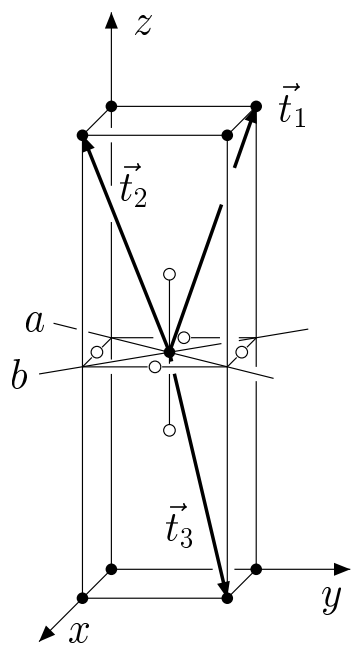

FIG. 1: Structure of tetragonal La_2CuO_4, showing the basic translations of the Bravais lattice $\vec{t}_q$. The space group is $I4/mmm$. Open circles are O, solid are Cu. La is not shown.

1.2. Magnetic and superconducting bands

An energy band is called "magnetic band with the magnetic group M" if the Bloch functions of this band can be unitarily transformed into Wannier functions which are

centered on the atomic positions;

Electronic address: krueger@mfm.pg.de

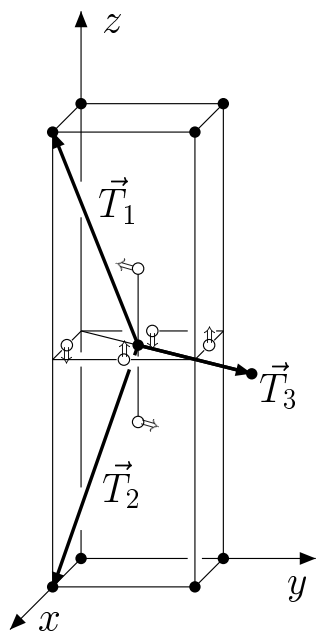

FIG. 2: Structure of orthorhombic La_2CuO_4 with the space group Cmca, showing the basic translations of the Bravais lattice $\overset{b}{\circ}$. Open circles are O, solid are Cu. La is not shown. The arrows * indicate the distortions of the O atoms.

symmetry-adapted to M ; and

optimally localizable.

"Optimally localizable" means that the Wannier functions are as well localizable as possible. Observations on the band structures of Fe [4] and Cr [5] suggest that in both Fe and Cr a narrow, roughly half-filled magnetic band is responsible for the stability of the ferromagnetic and the (antiferromagnetic) spin-density wave state, respectively, in these materials. This observation can be interpreted within a nonadiabatic extension of the Heisenberg model, the "nonadiabatic Heisenberg model" (NHM) [6].

An energy band is called "superconducting band" if the Bloch functions of this band can be unitarily transformed into spin-dependent Wannier functions which are

centered on the atomic positions;

symmetry-adapted to the space group of the considered material; and

optimally localizable.

Observations on the band structures of a great number of elemental metals suggest that narrow, roughly half-filled superconducting bands are responsible for the stability of superconducting states. Also this observation can be interpreted within the NHM [7, 8, 9].

Optimally localizable and symmetry-adapted Wannier functions are defined in Appendix B. The small irreducible representations of all the magnetic or superconducting energy bands in the space groups of La_2CuO_4 are listed in Tables XI – XVI at the end of this paper. The way to determine these symmetry labels is also summarized in Appendix B.

1.3. Nonadiabatic Heisenberg model

Within the NHM, the electrons in narrow, half-filled bands may lower their Coulomb energy by occupying an atomiclike state as defined by Mott [10] and Hubbard [11]: the electrons occupy as long as possible localized states and perform their band motion by hopping from one atom to another. The Hamiltonian H^n within the NHM is distinguished from any adiabatic Hamiltonian by a particular feature: the symmetry of H^n depends on the symmetry of the localized functions representing the localized states. As a consequence, within this model the localized states must be represented by optimally localizable Wannier functions which are adapted to the symmetry of the considered phase. These Wannier functions may be usual (spin-independent) or spin-dependent Wannier functions.

Spin-independent Wannier functions are related to magnetic bands, and, for the first time in this paper, to a "neutral" band. In an atomiclike state represented by spin-dependent Wannier functions, the conservation of crystal spin requires a strong coupling between the electron spins and the crystal spins of suitable boson excitations. Below a transition temperature, this spin-boson interaction leads to stable Cooper pairs.

The mechanism of Cooper pair formation within such an atomiclike system resembles the familiar BCS mechanism [12]. However, the Cooper pairs are stabilized in a new way by constraining forces. Though these constraining forces neither are considered within the original BCS theory nor within the modern theory of superconductivity, it cannot be excluded that they must operate in superconducting states because electrons forming Cooper pairs possess only half of the degrees of freedom of free electrons.

The above mentioned "suitable bosons" are boson excitations bearing the crystal-spin angular momentum 1 ~ and being sufficiently stable to carry it through the crystal. The order of magnitude of the superconducting transition temperature is determined by the excitation energy of those stable crystal-spin-1 bosons of the crystal which have the lowest excitation energy [13].

All the Wannier functions considered in this paper are centered at the Cu atoms because La_2CuO_4 has a single conduction band [6].

2. CONDUCTION BAND OF TETRAGONAL La_2CuO_4

Tetragonal La_2CuO_4 possesses a pronounced conduction band characterized by the small representations

$$Z_1^+;\ {}_2;X_3^+;P_3;\text{ and }N_1^+; \qquad (1)$$

see Fig. 3.

2.1. Exclusion of a neutral atomiclike state with usual Wannier functions

Band (1) is not listed in Table XI. Hence, in the tetragonal phase of La_2CuO_4 the electrons of this band cannot lower their Coulomb energy by occupying an atomiclike state because suitable symmetry-adapted and optimally localizable Wannier functions do not exist.

2.2. Exclusion of a superconducting band

Taking into account the electron spin, the conduction band (1) is characterized by the double-valued small representations

$$Z_6^+;\ {}_6;X_5^+;P_7;\text{ and }N_3^+ + N_4^+; \qquad (2)$$

see Table IX. This band is not a superconducting band because it is not listed in Table XII. Hence, the electrons of this band cannot lower their Coulomb energy by occupying an atomiclike state even if the Wannier functions representing the localized states are allowed to be spin-dependent. Thus, in the framework of the NHM we cannot expect stable Cooper pairs in the tetragonal phase of La_2CuO_4.

3. EXCLUSION OF AN ANTIFERROMAGNETIC BAND WITH THE SPACE GROUP OF ANTIFERROMAGNETIC CHROMIUM

Folding the conduction band (1) into the Brillouin zone of antiferromagnetic Cr (as given, e.g., in Fig. 3 of Ref. [15]), the band becomes characterized by the small representations

$${}_2^+ + {}_2;M_{20};A_{10};\text{ and }R_5; \qquad (3)$$

see Table VII. This band is not listed in Table XV. Hence, optimally localizable Wannier functions being adapted to P4=mnc do not exist. The electrons cannot lower their Coulomb energy by occupying an atomiclike state represented by such antiferromagnetic Wannier functions. Hence, a spin structure with the space group P4=mnc (that means, with the spins lying parallel to the z axis in Fig. 1) is not predicted within the NHM.

4. CONDUCTION BAND OF ORTHORHOMBIC La_2CuO_4

In the tetragonal phase of La_2CuO_4, it is the symmetry of the Bloch functions at point which does not allow the construction of symmetry-adapted and optimally localizable (spin-dependent) Wannier functions: the Bloch functions at are negative with respect to the inversion, but at the other points of symmetry they are positive.

In the orthorhombic phase of La_2CuO_4 the oxygen atoms are slightly displaced from their tetragonal positions [2], see Fig. 2. In the Brillouin zone of this phase, the tetragonal points and X become equivalent, see Fig. 4. Hence, in the orthorhombic Brillouin zone we may replace the unsuited Bloch functions at the tetragonal point by suited Bloch functions coming from the tetragonal point X, if they exist. In fact, there exist well-suited functions at the tetragonal point X which are positive with respect to the inversion and have nearly the same energy as the functions at the tetragonal points and Z. These are the Bloch functions with X_2^+ and X_4^+ symmetry, see Fig. 3.

We get the "active band" denoted in Fig. 5 by the bold line if we replace the tetragonal Z_1^+ and ${}_2$ functions by the tetragonal X_2^+ and X_4^+ functions. This band is proposed to be responsible for the physical properties of La_2CuO_4. Symmetry-adapted Wannier functions constructed from the Bloch functions of the active band represent localized states with orthorhombic symmetry. However, we may assume that these orthorhombic states do not strongly differ from states with tetragonal symmetry, i.e., we may assume that these orthorhombic states are states of slightly distorted tetragonal symmetry. This is because, first, the predominant portion of the Bloch functions of this band comes from the Bloch functions of the initial tetragonal band (1), and, second, the new tetragonal X functions have nearly the same energy as the initial tetragonal Z and functions.

The active band in the orthorhombic structure is characterized by the representations

$${}_2^+ + {}_3^+;Y_2^+ + Y_3^+;R_1^+ + R_2^+;T_2\text{ and }Z_2; \qquad (4)$$

where ${}_2^+$ comes from the tetragonal X_2^+ state, ${}_3^+$ comes from X_3^+, Y_2^+ comes from X_4^+, Y_3^+ comes from X_3^+, too, $R_1^+ + R_2^+$ comes from N_1^+, and T_2 and Z_2 come from states at the tetragonal U and lines, respectively, see Table VI.

Band (4) is identical to band 2 in Table XIV. Hence, the Bloch functions of this band can be unitarily transformed into optimally localizable Wannier functions symmetry-adapted to the space group Cmca. The electrons of this band may lower their Coulomb energy by occupying an atomiclike state represented by these Wannier functions. However, the related nonadiabatic Hamiltonian H^n has no longer the symmetry of the tetragonal space group I4=mmm since it commutes only with those space group operators of the tetragonal group I4=mmm which also belong to the subgroup Cmca. Therefore,

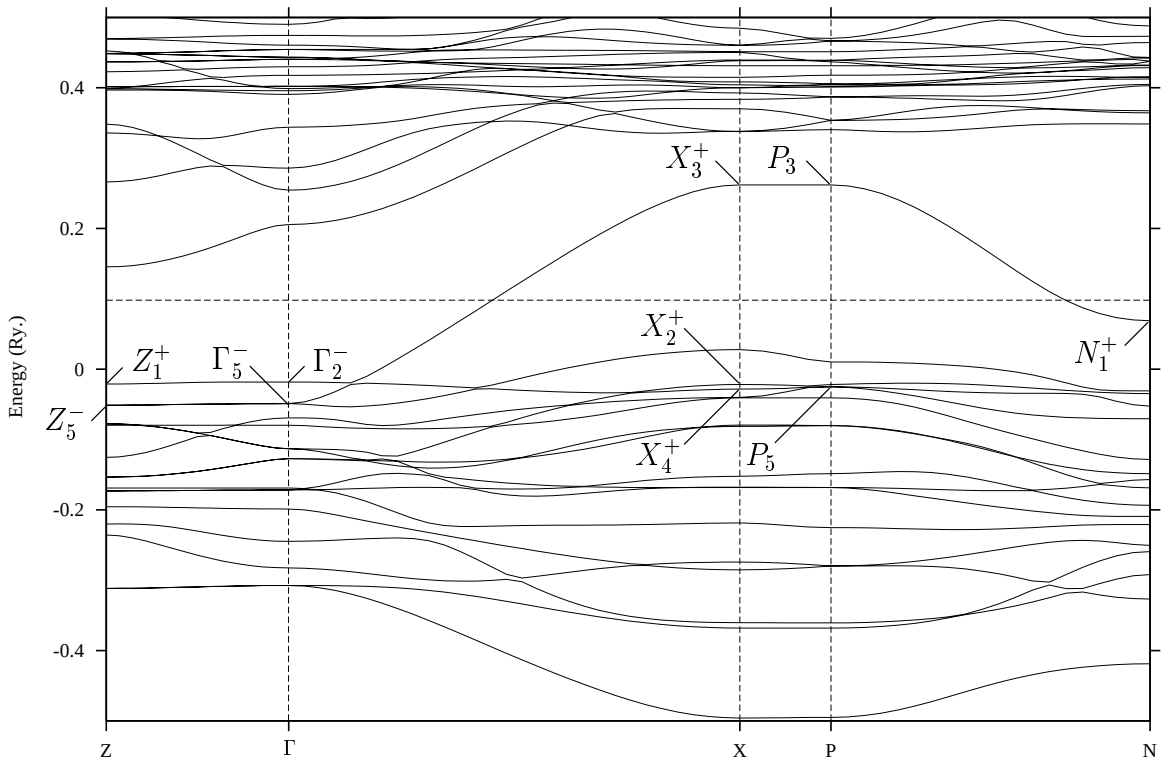

FIG. 3: Band structure of tetragonal La_2CuO_4 as calculated by Ove Jepsen [14], with symmetry labels determined by the author. The band characterized by Z_1^+, $_2$ (or Z_5, $_5$), $X_3^+ + X_2^+$, $P_3 + P_5$, and N_1^+ forms a natural narrow conduction band. However, the electrons of this nearly half- lled band cannot occupy the (energetically favorable) atomiclike state because suitable symmetry-adapted and optimally localizable Wannier functions do not exist in the tetragonal phase. However, when the bands are folded into the Brillouin zone of the orthorhombic phase (see Fig. 5), the points X and become equivalent. In the new Brillouin zone we may replace the Z_1^+ and $_2$ Bloch functions by the X_2^+ and X_4^+ functions of nearly the same energy. With these new functions, the construction of symmetry-adapted Wannier becomes possible.

such an atomiclike state represented by Wannier functions of reduced symmetry requires a change of the symmetry of the crystal.

4.1. Antiferromagnetic band with the orthorhombic space group Cmca

The space group Cmca is the space group of the antiferromagnetic structure depicted in Fig. 6. Thus, the electrons might occupy an atomiclike state by putting their spins antiparallel as shown in Fig. 6. This appears to be possible, because the Wannier functions of band 2 in Table XIV can be constructed in such a way that they are symmetry-adapted to the whole magnetic group

$$M = Cmca + \{K \mid \tfrac{1}{2}\tfrac{1}{2}\tfrac{1}{2}\}Cmca; \qquad (5)$$

where K denotes the operator of time-inversion, see Appendix B. In this case, no spatial distortion of the tetragonal lattice would be required, since the spin structure by itself together with the accompanying magnetostriction represents a change of the tetragonal symmetry.

However, within the NHM stable spin structures with the space group Cmca do not exist because M does not possess suitable corepresentations, see Appendix A.

4.2. Spatially distorted crystal with the orthorhombic space group Cmca

Hence, the electrons can occupy the energetically favorable atomiclike state only in a spatially distorted crystal. Therefore, the system produces the experimentally established distortion with the space group Cmca. This is possible because of the favorable position of the oxygen atoms: suitable displacements of these atoms also produce a crystal with the antiferromagnetic space group Cmca. Within the distorted system, there exist three di erent atomiclike states.

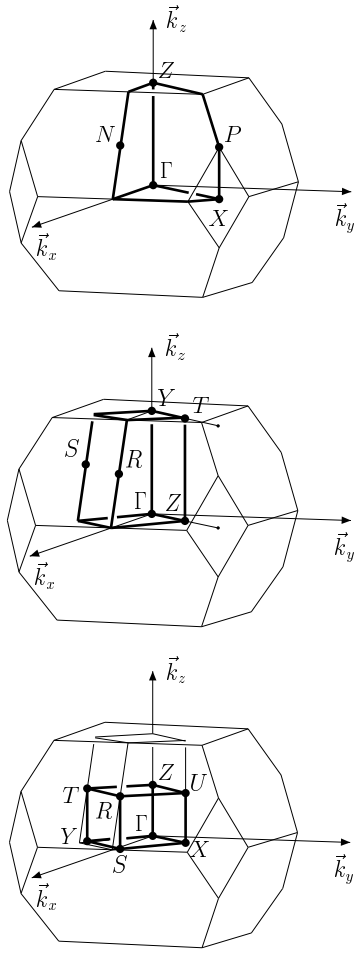

FIG. 4: Brillouin zones of La_2CuO_4.
Top: Brillouin zone of the tetragonal space group I4/mmm with the Bravais lattice $^{v}_{q}$, as given in Fig. 3.10 (b) of Ref. [16].
Center: Basic domain of the Brillouin zone of the orthorhombic space group Cmca with the Bravais lattice $^{b}_{o}$ within the Brillouin zone of $^{v}_{q}$.
Bottom: Basic domain of the Brillouin zone of the space group Pccn of the antiferromagnetic phase with the Bravais lattice $_{o}$ within the basic domain of the Brillouin zone of $^{b}_{o}$.

4.2.1. Neutral band

The Wannier functions of band 2 in Table XIV may also be constructed so that they are symmetry-adapted to the grey magnetic group

$$M = Cmca + K \quad Cmca: \tag{6}$$

Thus, in this spatially distorted crystal the conduction electrons can occupy a "neutral" atomiclike state represented by these spin-independent Wannier functions being invariant under time-inversion. I believe that this neutral state is responsible for the phase of $La_{2\ x}Sr_xCuO_4$ which is neither antiferromagnetic nor superconducting.

4.2.2. Antiferromagnetic band with the space group Pccn of the experimentally established antiferromagnetic structure

The experimentally established [1] antiferromagnetic structure of La_2CuO_4 with the space group Pccn is depicted in Fig. 7. Folding the active band (4) into the Brillouin zone of Pccn (given in Fig. 4), we get a band consisting of four branches which is characterized by the representations

$$\begin{gathered} {}^{+}_{1} + {}^{+}_{2} + {}^{+}_{3} + {}^{+}_{4}; R^{+}_{1} + R^{+}_{2} + R^{+}_{3} + R^{+}_{4}; \\ Y_1 + Y_2; X_1 + X_2; Z_1 + Z_2; \\ U_1 + U_2; T_1 + T_2; \text{ and } S_1 + S_2; \end{gathered} \tag{7}$$

see Table VIII. This band is identical to band 1 in Table XVI. Hence, the Bloch functions of this band can be unitarily transformed into optimally localizable Wannier functions symmetry-adapted to the space group Pccn. Thus, within the NHM the electrons may lower their Coulomb energy by producing the antiferromagnetic structure shown in Fig. 7. However, this spin structure is connected with the experimentally established spatial distortion of the tetragonal lattice because the spin structure alone does not produce a crystal with the space group Pccn.

Fig. 7 suggests that the related magnetic group may either be written as

$$M = Pccn + fK \ \tfrac{1}{2}\tfrac{1}{2}0gPccn \tag{8}$$

or

$$M = Pccn + fK \ \tfrac{1}{2}0\tfrac{1}{2}gPccn; \tag{9}$$

where still K denotes the operator of time-inversion.

The first magnetic group (8) possesses suitable corepresentations and, hence, spin structures with this group can be stable within the NHM, see Appendix A.

4.2.3. Superconducting band

Taking into account the electron spin, the active band (4) is characterized by the double-valued representations

$$2\ {}^{+}_{5}; 2Y^{+}_{5}; 2R^{+}_{3} + 2R^{+}_{4}; T_3 + T_4 \text{ and } Z_3 + Z_4; \tag{10}$$

see Table X. This band is identical to band 1 in Table XIII. Hence, the Bloch functions of this band can be unitarily transformed into optimally localizable spin-dependent Wannier functions symmetry-adapted to the space group Cmca. The electrons may lower their Coulomb energy by occupying an atomiclike state represented by these spin-dependent Wannier functions. In this case, the conservation of crystal spin requires a strong coupling between the electron spins and the crystal spins of suitable boson excitations. Below a transition temperature, this coupling leads to a superconducting state. However, this superconducting state exists only in the space group Cmca and hence, is connected with the experimentally established spatial distortion of the tetragonal lattice.

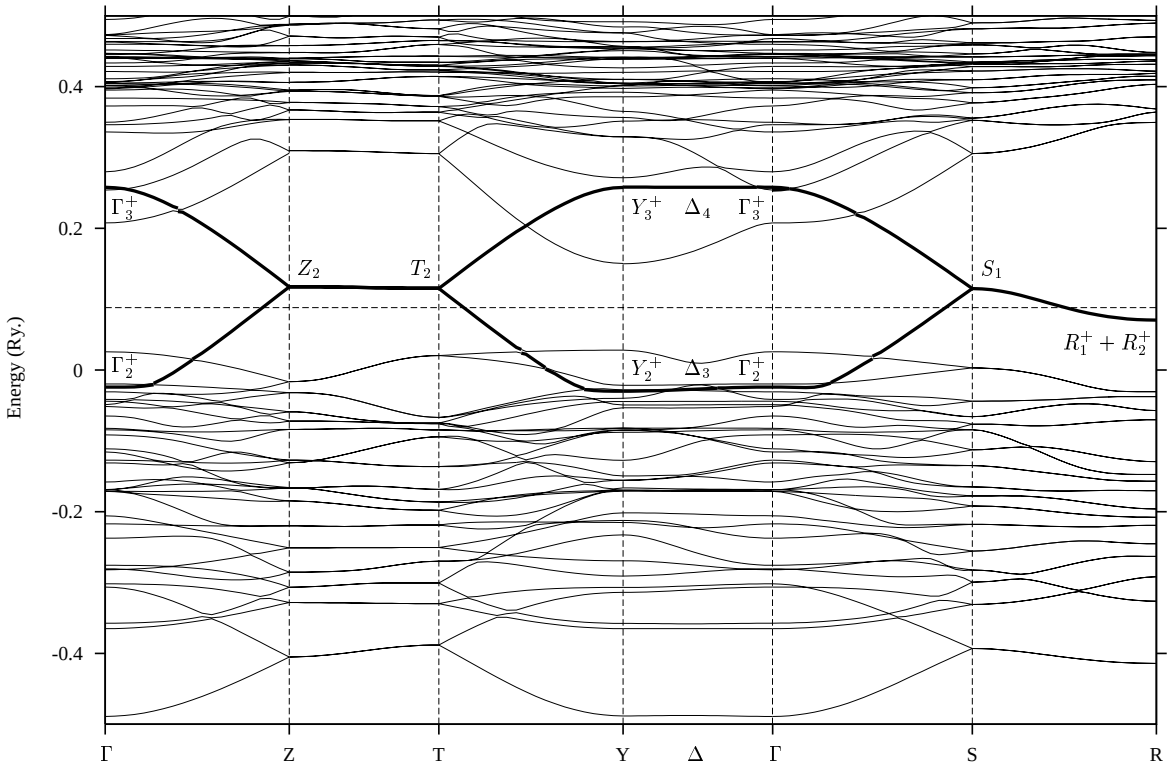

FIG. 5: Band structure of orthorhombic La_2CuO_4 as calculated by Ove Jepsen [14], with symmetry labels determined by the author. The bold line shows the "active band" which is proposed to be responsible for the physical properties of La_2CuO_4. The electrons of this band could occupy an energetically favorable atomiclike state by putting their spins antiparallel as shown in Fig. 6. Such a spin structure with the space group Cmca would not require any distortion of the tetragonal lattice. However, this spin structure is not stable because the related magnetic group does not possess suitable corepresentations. Alternatively, the electrons may occupy an atomiclike state either by producing the experimentally established spin structure with the space group Pccn, a "neutral" atomiclike state invariant under time-inversion (and hence, without any spin structure) or a superconducting state, all of them being stable only in a (slightly) distorted lattice with the orthorhombic space group Cmca.

5. SUMMARY AND DISCUSSION

5.1. Pure La_2CuO_4

The symmetry of the optimally localizable Wannier functions in the conduction band of La_2CuO_4 suggests that some aspects of the physical properties of this compound can be understood within the NHM in terms of magnetic, neutral, and superconducting bands.

The conduction band of tetragonal La_2CuO_4 is clearly an "antiferromagnetic" band tending to produce the antiferromagnetic structure with the space group Cmca illustrated in Fig. 6. The conduction electrons would be able to occupy an atomiclike state by producing this spin structure without any additional spatial distortion of the tetragonal crystal. However, the nonadiabatic Hamiltonian H^n does not possess antiferromagnetic eigenstates with the space group Cmca because the related magnetic group has no suitable corepresentations.

Thus, the system is forced to produce a spatial distortion of the crystal so the conduction electrons can occupy the energetically favorable atomiclike state. We recognize the intention of the nature to stabilize the atomiclike state with the least possible distortion: the positions of the oxygen atoms are shifted in a subtle manner in order that the basic translation $\vec{t}_3$ (see Fig. 1) in the tetragonal lattice becomes doubled while the other two basic translations $\vec{t}_1$ and $\vec{t}_2$ still connect two lattice points. This slightly distorted crystal has the experimentally established orthorhombic space group Cmca, that is, the same space group as the spin structure in Fig. 6. Within the distorted system, the conduction electrons now have three possibilities to condense into an atomiclike state.

First, in the orthorhombic crystal the Bloch functions of the conduction band can be unitarily transformed into optimally localizable Wannier functions adapted to the symmetry of the experimentally established spin structure (depicted in Fig. 7) with the space group Pccn. In this case, the related magnetic group [given in Eq. (8)] possesses suitable corepresentations in order that H^n has eigenstates with this spin structure. Therefore, the electrons may occupy the energetically favorable atomi-

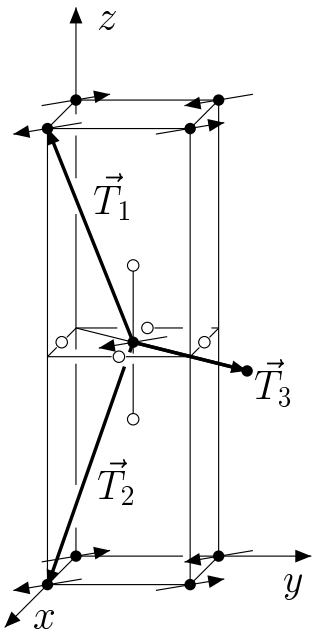

FIG. 6: Hypothetical spin structure of La_2CuO_4 with the space group Cmca. However, this spin structure is not stable because the related magnetic group does not possess suitable corepresentations.

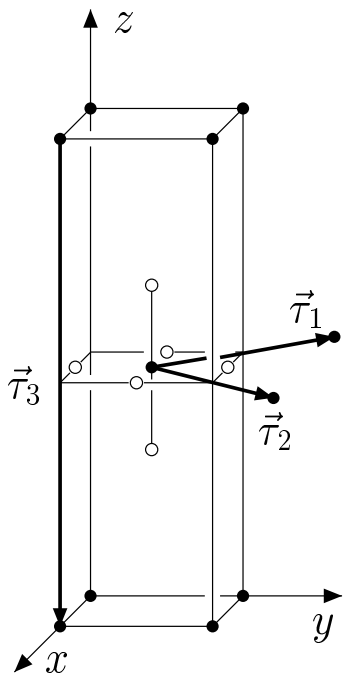

FIG. 8: Basic translations of the Bravais lattice $_o$ of the experimentally established spin structure of La_2CuO_4 shown in Fig. 7.

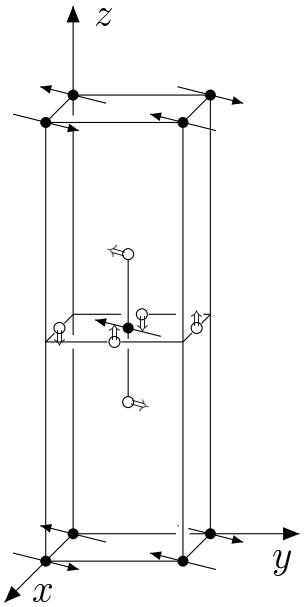

FIG. 7: Experimentally established [1] spin structure of La_2CuO_4 with the space group Pccn. Open circles are O, solid are Cu. La is not shown. The arrows * indicate the distortions of the O atoms.

clike state by producing this antiferromagnetic structure. However, it is the spatial orthorhombic distortion of the crystal which stabilizes the antiferromagnetic structure.

Secondly, the orthorhombic distortion of the crystal need not be accompanied by a spin structure. In the distorted system there exist optimally localizable (usual) Wannier functions which are adapted to the orthorhombic symmetry. I believe that the "neutral" atomiclike state represented by these Wannier functions is responsible for the "spin-glass" phase [1] of doped La_2CuO_4 because this phase neither is antiferromagnetic nor is superconducting. However, the question why such a neutral state has features of spin-glass systems [3], requires further investigation. Also in this case, it is the experimentally established orthorhombic distortion which stabilizes the neutral phase.

Thirdly, in the orthorhombic system the conduction electrons may occupy an atomiclike state represented by spin-dependent Wannier functions. In such an atomiclike state, the conservation of crystal spin requires a strong coupling between the electron spins and the crystal spins of stable crystal-spin-1 boson excitations. Below a transition temperature T_c, this spin-boson interaction leads to the formation of Cooper pairs. Also this spin-boson phase is not stable in the tetragonal system but is stabilized by the orthorhombic distortion.

Most likely, in any material the stable crystal-spin-1 bosons of lowest excitation energy are coupled phonon-

plasmon modes. In the isotropic lattices of the transition elements they have dominant phonon character. However, phonon-like excitations are not able to transport crystal-spin angular-momenta within the two-dimensional copper-oxygen layers of La_2CuO_4 [13]. Thus, in the spin-boson phase the electron spins interact with boson excitations of dominant plasmon character. The relatively high energy of these plasmon-like crystal-spin-1 bosons is proposed to be responsible for the high superconducting transition temperature observed in the doped material.

5.2. Doped $La_{2-x}Sr_xCuO_4$

In doped $La_{2-x}Sr_xCuO_4$ the symmetry of the crystal is disturbed and all the statements in the preceding section are, strictly speaking, no longer valid. However, we may assume that for small values of x the given description of the atomiclike states holds also in the doped system because the symmetry of the physically relevant copper-oxygen layers is not seriously affected by the doping.

In doped $La_{2-x}Sr_xCuO_4$, all three possible atomiclike states described in the preceding section are evidently realized: for $0 \quad x < 0.015$ the antiferromagnetic state has the lowest energy, then a neutral phase is stable and above $x \quad 0.05$ the material becomes superconducting [1]. I propose a simple model which might help to understand this x dependence of the physical properties of $La_{2-x}Sr_xCuO_4$:

At the transition from the adiabatic to the nonadiabatic system (i.e., at the transition from a purely bandlike to the atomiclike state), the total energy of the electron system decreases by the "condensation energy"

$$E_i(x) = E_i^e \quad E_i^d(x); \tag{11}$$

where i = 1, 2, and 3 labels the antiferromagnetic, the neutral, and the spin-boson phase, respectively. (Below the transition temperature, the latter phase is superconducting.)

E_i^e stands for the electronic part of the condensation energy. It is defined in Eqs. (2.20) and (5.3) of Ref. [6] for the superconducting and magnetic state, respectively, and may be assumed to be independent of the Sr concentration x since the physically relevant copper-oxygen planes are not seriously affected by the doping.

Atomiclike states in La_2CuO_4 require an orthorhombic distortion of the tetragonal crystal. Hence, the total condensation energy $E_i(x)$ decreases by the energy $E_i^d(x)$ required to distort the tetragonal crystal. The x-dependence of this "distortion energy" might be understood on the basis of the following assumptions.

With increasing x the translation symmetry of the crystal is increasingly disturbed and the points and X in the tetragonal Brillouin zone become increasingly equivalent. As a consequence, the orthorhombic distortion that is required for that and X are (completely) equivalent, becomes smaller with increasing x (and disappears completely for $x \quad 0.2$). Thus, for fixed i, the required distortion energy $E_i^d(x)$ decreases with increasing x:

$$E_i^d(x_1) > E_i^d(x_2) \quad \text{if} \quad x_1 < x_2: \tag{12}$$

On the basis of this assumption, the experimental results may be interpreted by assuming that, first, the purely electronic condensation energy is maximum for the spin-boson and minimum for the antiferromagnetic state,

$$E_1^e < E_2^e < E_3^e; \tag{13}$$

and that, second, for fixed x, the required distortion energy is also maximum for the spin-boson and minimum for the antiferromagnetic state,

$$E_1^d(x) < E_2^d(x) < E_3^d(x): \tag{14}$$

Under these assumptions, the system undergoes the phase transitions in order that the condensation energy is maximum at any Sr concentration x, see Fig. 9.

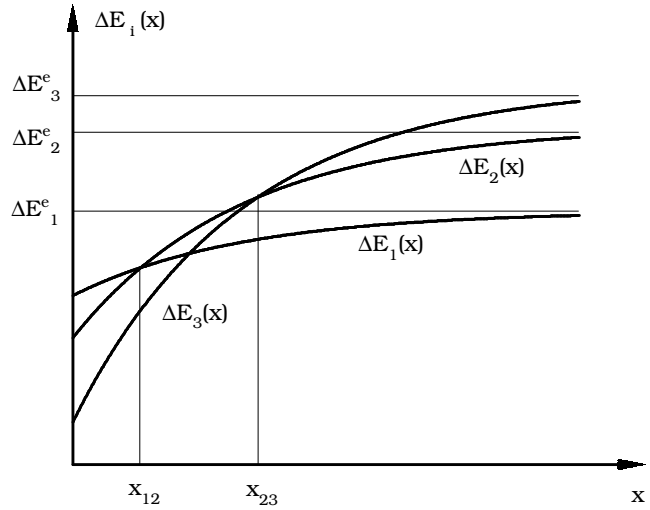

FIG. 9: Qualitative plot of the condensation energy $E_i(x)$ [given in Eq. (11)] as a function of the Sr concentration x within the simple model defined by the three assumptions (12), (13), and (14). i = 1, 2, and 3 labels the antiferromagnetic, the neutral, and the spin-boson phase, respectively. The condensation energy is maximum for any concentration, if the phase transitions from the antiferromagnetic to the neutral and from the neutral to the spin-boson phase occur at the Sr concentrations x_{12} and x_{23}, respectively. Below a transition temperature, the spin-boson phase is superconducting.

The first assumption (13) is in accordance with my observations on the elemental metals, see Sec. V of Ref. [4]. The second assumption is corroborated by the fact that a spin structure alone (together with the related magnetostriction) represents a distortion of the lattice without any spatial distortion. Hence, it is conceivable that the required spatial distortion of the tetragonal crystal is smallest in the antiferromagnetic state.

APPENDIX A: STABLE MAGNETIC STATES

Consider a magnetic state $|m\rangle$ and the related magnetic group

$$M = H + AH; \tag{A1}$$

where H denotes the space group and A stands for any anti-unitary element of M. In the case of the spin structure depicted in Fig. 6, we have $H = Cmca$ and may choose $A = \{K|\frac{1}{2}\frac{1}{2}\frac{1}{2}\}$ with K denoting the operator of time-inversion.

Within the NHM, both the magnetic state $|m\rangle$ and the time-inverted state

$$\overline{|m\rangle} = K|m\rangle$$

are eigenstates of the nonadiabatic Hamiltonian H^n. Therefore, standard group-theoretical methods can be applied to magnetic states, too. A stable magnetic state $|m\rangle$ complies with two conditions:

- $|m\rangle$ is basis function of a one-dimensional corepresentation of M;
- $|m\rangle$ and the time-inverted state $\overline{|m\rangle}$ are basis functions of a two-dimensional irreducible corepresentation of the gray magnetic group

$$\overline{M} = M + KM; \tag{A2}$$

see Sec. III.C of Ref. [5].

Consequently, a stable magnetic state can exist in the space group H if H has at least one one-dimensional single-valued representation R following

- case (a) with respect to the magnetic group $H + AH$ and
- case (c) with respect to the magnetic group $H + KH$.

The cases (a) and (c) are defined in Eqs. (7.3.45) and (7.3.47), respectively, in the textbook of Bradley and Cracknell [16]. The irreducible corepresentation derived from R stays one-dimensional in case (a) and becomes two-dimensional in case (c).

1. Space group Cmca

Table II lists all the irreducible representations of the space group $H = Cmca$ of orthorhombic La_2CuO_4. The second and third column of this Table specify whether the corepresentation of $H + KH$ and $H + \{K|\frac{1}{2}\frac{1}{2}\frac{1}{2}\}H$, respectively, derived from the given representation R follows case (a) or case (c).

The only one-dimensional representations which apparently comply with the above condition for a stable antiferromagnetic state are the small representations at point R. However, the little group at R is not the complete space group. Therefore, a stable antiferromagnetic state with the space group $Cmca$ does not exist.

2. Space group Pccn

Table III lists all the irreducible representations of the space group $H = Pccn$. The second, third, and fourth column of this table specify whether the corepresentation of $H + KH$; $H + \{K|\frac{1}{2}\frac{1}{2}0\}H$; and $H + \{K|\frac{1}{2}0\frac{1}{2}\}H$ [cf. Eqs. (8) and (9)], respectively, derived from the given representation R follows case (a) or case (c).

For the group $H + \{K|\frac{1}{2}0\frac{1}{2}\}H$ there do not exist suitable representations. However, for the group $H + \{K|\frac{1}{2}\frac{1}{2}0\}H$ all the small representations at point R comply with the above condition for a stable antiferromagnetic state. Since now the little group at R includes all the space-group elements, a stable antiferromagnetic state with the space group $Pccn$ is possible.

APPENDIX B: OPTIMALLY LOCALIZABLE AND SYMMETRY-ADAPTED WANNIER FUNCTIONS

1. Usual (spin-independent) Wannier functions

Consider a subgroup H of the space group $I4/mmm$ of La_2CuO_4 and assume the energy bands (or a part of the energy bands) of La_2CuO_4 to be folded into the Brillouin zone B_H of H. Let be the number of Cu atoms in the unit cell of H and consider single energy bands in B_H. Assume the Bloch functions $\varphi_{\vec{k}q}(\vec{r})$ (with the wave vector $\vec{k}$) of this "energy band with branches" to be unitarily transformed into Wannier functions

$$w_i(\vec{r} - \vec{T} - \vec{\tau}_i) = \frac{1}{\sqrt{\ }} \sum_{\vec{k}} \sum_{q=1}^{\ } e^{i\vec{k}(\vec{T}+\vec{\tau}_i)} g_{iq}(\vec{k}) \varphi_{\vec{k}q}(\vec{r}) \tag{B1}$$

centered at the Cu atoms. The first sum in this equation runs over the vectors $\vec{k}$ of the first Brillouin zone (BZ), the second sum runs over the branches, $\vec{T}$ and $\vec{\tau}_i$ denote the vectors of the Bravais lattice and the positions of the Cu atoms within the unit cell, respectively, and the coefficients $g_{iq}(\vec{k})$ are the elements of a unitary matrix $g(\vec{k})$,

$$g^{-1}(\vec{k}) = g^{\dagger}(\vec{k}). \tag{B2}$$

The Wannier functions are called "optimally localizable" if the Bloch-like functions

$$\tilde{\varphi}_{\vec{k}i}(\vec{r}) = \sum_{q=1}^{\ } g_{iq}(\vec{k}) \varphi_{\vec{k}q}(\vec{r}) \tag{B3}$$

are (for fixed $\vec{r}$) continuous functions of $\vec{k}$ everywhere in the reciprocal space. Fortunately, the question whether or not the functions $\tilde{\varphi}_{\vec{k}i}(\vec{r})$ vary continuously through the planes of symmetry within or on the surface of the Brillouin zone, can be treated by group theory [17, 18].

The main result is the relatively simple criterion given in Eq. (B7).

The Wannier functions are called "symmetry-adapted to H" if they satisfy the equation

$$P(a)w_i(\vec{r}-\vec{T}-\vec{\sigma}_i)=\sum_{j=1}^{X}D_{ji}(\ )w_j(\vec{r}-\vec{T}-\vec{\sigma}_j) \quad (B4)$$

by application of the operators $P(a)$ of H,

$$a=\{\ |\vec{t}\}\in H; \quad (B5)$$

see Appendix A of Ref. [6]. The matrices $D_0(\ )=[D_{ji}(\ )]$ form a (reducible or irreducible) single-valued representation D_0 of the point group H_0 of H. The sum on the right hand side of Eq. (B4) consists of one summand only because there is one Wannier function at each atom. Hence, the matrices $D_0(\ )$ have only one non-vanishing element, say $d_{ji}(\ )$, in each row and each column. The non-vanishing diagonal elements $d_{jj}(\ )$ are equal to $_0(\ )$ and the other non-vanishing elements may also be chosen to be equal to $_0(\ )$, so that we have

$$d_{ji}(\ )=\ _0(\ ) \quad (B6)$$

for all the non-vanishing elements of $D_0(\ )$, where $_0(\ )$ stands for the character of the one-dimensional representation d_0 of H_0 used in the following Eq. (B7).

Suppose the symmetry of the Bloch functions in the Brillouin zone B_H of H to be determined by the compatibility relations given in the Tables VI–VIII. At each point of symmetry $P_{\vec{k}}$ of B_H the Bloch functions of the branches of the band belong to a -dimensional single-valued small representation $D_{\vec{k}}$ of the little group $H_{\vec{k}}$ of $P_{\vec{k}}$. $D_{\vec{k}}$ may be irreducible or is the direct sum over small irreducible representations of $H_{\vec{k}}$.

The coefficients $g_{iq}(\vec{k})$ can be chosen so that the Wannier functions in Eq. (B1) are optimally localizable and symmetry-adapted to H if and only if the equation

$$_{\vec{k}}(a)=\ _0(\ )e^{i\ \vec{k}\vec{t}}\sum_{i=1}^{X}n_i(a)e^{i\vec{s}_i(\vec{k}-\ \vec{k})} \quad (B7)$$

is satisfied at each $P_{\vec{k}}$ of B_H and for each element $a=\{\ |\vec{t}\}$ in the little group $H_{\vec{k}}$. $_{\vec{k}}(a)$ denotes the character of the representation $D_{\vec{k}}$, $_0(\ )$ stands for the character of any one-dimensional single-valued representation d_0 of the point group H_0 of H, and

$$n_i(a)=\begin{cases}1 & \text{if } \vec{s}_i+\vec{t}=\vec{s}_i+\vec{T}\\ 0 & \text{else}\end{cases} \quad (B8)$$

with $\vec{T}$ being a vector of the Bravais lattice. This Eq. (B7) is derived from Eqs. (1.8) and (4.28) of Ref. [17] (see also Sec. 3 of Ref. [18]). It is satisfied for all $a\in H_{\vec{k}}$ if it is satisfied for one element of each class of $H_{\vec{k}}$.

2. Spin-dependent Wannier functions

The Wannier functions given in Eq. (B1) become spin-dependent if the Bloch functions $'_{\vec{k}q}(\vec{r})$ in this equation are allowed to have $\vec{k}$-dependent spin-directions, see Eqs. (A21) and (A22) in Ref. [6]. Also energy bands with optimally localizable and symmetry-adapted spin-dependent Wannier functions situated at the Cu atoms follow Eq. (B7). In this case, however, $D_{\vec{k}}$ is a 2 -dimensional double-valued representation and $_0(\ )$ denotes the character of any two-dimensional double-valued representation d_0 of H_0.

3. Magnetic groups

The Wannier functions given in Eq. (B1) are called symmetry-adapted to the antiferromagnetic group

$$M=H+\{K|\vec{\sigma}\}H \quad (B9)$$

if the equation

$$KP\{E|\vec{\sigma}\}w_i(\vec{r}-\vec{T}-\vec{\sigma}_i)=\sum_{j=1}^{X}N_{ji}w_j(\vec{r}-\vec{T}-\vec{\sigma}_j) \quad (B10)$$

is satisfied in addition to Eq. (B4), where K still denotes the operator of time-inversion. Since there is one Wannier function at each atom, also the matrix $N=[N_{ji}]$ has only one non-vanishing element, say n_{ji}, in each row and each column which may be put equal to one,

$$n_{ji}=1: \quad (B11)$$

Suppose that in Eq. (B10) we obtain the Wannier function w_j by application of the operator $KP\{E|\vec{\sigma}\}$ on the function w_i. Then conversely we obtain the function w_i applying this operator on w_j. This is because 2 is a vector of the Bravais lattice,

$$2\vec{\sigma}=\vec{T}; \quad (B12)$$

and hence from $\vec{\sigma}_i+\vec{\sigma}=\vec{\sigma}_j+\vec{T}_1$ it follows $\vec{\sigma}_j+\vec{\sigma}=\vec{\sigma}_i+\vec{T}_2$, where $\vec{T}_1$ and $\vec{T}_2$ denote vectors of the Bravais lattice. Thus, the matrix N is symmetric,

$$n_{ji}=n_{ij}: \quad (B13)$$

N is the matrix representing K in the corepresentation of the point group

$$M_0=H_0+KH_0 \quad (B14)$$

of M which is derived from the representation D_0 of H_0 given in Eq. (B4). Hence, N must satisfy the equations

$$NN=1 \quad (B15)$$

and

$$D_0(\ )=ND_0(\ )N^{\ 1}\ \text{for}\ \ 2H_0; \quad (B16)$$

see Eq. (7.3.45) of Ref. [16]. The matrices $D_0(\ )$ are defined in Eq. (B4). [In Ref. [16] Eq. (7.3.45) is derived for irreducible representations. However, this derivation in Sec. 7.3 of Ref. [16] shows that Eq. (7.3.45) holds for reducible representations, too, if Eq. (B15) is satisfied.]

As a consequence of Eqs. (B11) and (B13), the first Eq. (B15) is satisfied (and hence $N = N\ \ = N^{-1}$). The validity of the second Eq. (B16) must be examined for each given magnetic group.

Assume Eq. (B7) to be valid in a given energy band. In Ref. [19] I have shown that then the coefficients $g_{iq}(\vec{k})$ [in Eq. (B1)] can be chosen so that the Wannier functions of this band are symmetry-adapted to the whole magnetic group M if the matrix N satisfies Eq. (B16) and the equation

$$S(\vec{K}) = N S(\vec{K}) N^{-1} e^{i\vec{K}} \qquad (B17)$$

for any vector $\vec{K}$ of the reciprocal lattice, where $S(\vec{K})$ is a -dimensional diagonal matrix with the elements

$$s_{jj} = e^{i\vec{K}\ \ \vec{\tau}_j}. \qquad (B18)$$

Using Eqs. (B11), (B12), and (B13) it can be verified that the matrix N defined by Eq. (B10) satisfies Eq. (B17). Thus, Eq. (B16) is the only additional condition for the existence of optimally localizable Wannier functions that are symmetry-adapted to the entire magnetic group M. This equation is satisfied for all the antiferromagnetic bands considered in this paper.

APPENDIX C: DESCRIPTION OF THE SPACE GROUPS

1. Tetragonal La_2CuO_4

Fig. 1 shows the basic translations of the space group $I4/mmm$ of tetragonal La_2CuO_4 and the Brillouin zone is drawn in Fig. 4 (top).

The point group D_{4h} consists of 16 elements,

$$\begin{aligned} D_{4h} = \{ & E; C_{4z}^{+}; C_{4z}; C_{2z}; C_{2x}; C_{2y}; C_{2a}; C_{2b}; I; \\ & S_{4z} = IC_{4z}^{+}; S_{4z}^{+} = IC_{4z}; \ _z = IC_{2z}; \ _x = IC_{2x}; \\ & \ _y = IC_{2y}; \ _{da} = IC_{2a}; \ _{db} = IC_{2b}\}; \end{aligned} \qquad (C1)$$

representing the identity operation, anti-clockwise and clockwise rotation through $\ /2$ radians about the z axis, rotation through $\ $ radians about the z, x and y axes, rotation through $\ $ radians about the a and b axes drawn in Fig. 1, and inversion. The following elements are products of the inversion with the former elements.

The space group $I4/mmm$ is symmorphic. Hence, all the point group elements are elements of $I4/mmm$, too.

2. Orthorhombic La_2CuO_4

The space group $Cmca$ of orthorhombic La_2CuO_4 has the basic translations shown in Fig. 2. The basic domain of the Brillouin zone of $Cmca$ is drawn in Fig. 4 (center).

Within the coordinate system given in Fig. 2 its point group is

$$D_{2h} = \{E; C_{2z}; C_{2a}; C_{2b}; I; \ _z; \ _{da}; \ _{db}\}. \qquad (C2)$$

In the space group $Cmca$ the 4 elements

$$C_{2z}; C_{2a}; \ _z; \text{ and } \ _{da} \qquad (C3)$$

are associated with the nonprimitive translation

$$(\tfrac{1}{2}\tfrac{1}{2}\tfrac{1}{2}).$$

3. Antiferromagnetic La_2CuO_4

Fig. 7 shows the spin structure of La_2CuO_4 as determined by Keimer et al. [1]. The space group is $Pccn$ with the Bravais lattice $_o$. Fig. 8 gives the basic translations as used in this paper, and the basic domain of the Brillouin zone is drawn in Fig. 4 (bottom).

The point group of the antiferromagnetic structure is also the group D_{2h} given in Eq. (C2). In the space group $Pccn$ the 2 elements

$$C_{2z} \text{ and } \ _z \qquad (C4)$$

are associated with the nonprimitive translation

$$(\tfrac{1}{2}\tfrac{1}{2}0);$$

the elements

$$C_{2a} \text{ and } \ _{da} \qquad (C5)$$

are associated with

$$(0\tfrac{1}{2}\tfrac{1}{2});$$

and the elements

$$C_{2b} \text{ and } \ _{db} \qquad (C6)$$

are associated with

$$(\tfrac{1}{2}0\tfrac{1}{2}).$$

APPENDIX D: TABLES

1. Irreducible representations

The irreducible representations given in Tables I – V (on the following pages) are determined by means of Tables 5.7 and 6.13 in the textbook of Bradley and Cracknell [16], with the notations of tables 5.8 and 6.14 in this book. The cases (a), (b), and (c) of the corepresentations follow Eqs. (7.3.45), (7.3.46), and (7.3.47) and are determined by Eq. (7.3.51) of Ref. [16].

2. Compatibility tables

Tables VI – VIII list compatibility relations between the points of symmetry in the Brillouin zone of a space group G and the related points of symmetry in the Brillouin zone of a subgroup H of G. These tables are determined in the way described in great detail in Ref. [15]. The compatibility relations between single-valued and double-valued representations given in Tables IX and X are determined by standard group-theoretical methods.

3. Antiferromagnetic, neutral, and superconducting bands

Tables XI, XIV, XV, and XVI list all the single-valued representations $D_{\vec{k}}$ with characters $_{\vec{k}}(a)$ satisfying Eq. (B7) in the space groups H = I4=mmm; Cmca; P4=mnc; and Pccn, respectively. Different bands belong to the character $_0(\ )$ of different one-dimensional representations d_0 of H_0. Tables XII and XIII list all the double-valued representations satisfying this equation with H = I4=mmm and Cmca, respectively. In this case, however, $D_{\vec{k}}$ is a 2 -dimensional double-valued representation and $_0(\ )$ denotes the character of any two-dimensional double-valued representation d_0 of H_0.

ACKNOWLEDGMENTS

I am very indebted to Ove Jepsen for providing me with all the data I needed to determine the symmetry of the Bloch functions in the band structure of La_2CuO_4. I thank Ernst Helmut Brandt for critical comments on the manuscript and continuing encouragement.

1. B. Keimer, N. Belk, R. J. Birgeneau, A. Cassanho, C. Y. Chen, M. Greven, M. A. Kastner, A. Aharony, Y. Endoh, R. W. Erwin, and G. Shirane, Phys. Rev. B 46, 14034 (1992).
2. R. J. Cava, A. Santoro, D. W. J. Jr., and W. W. Rhodes, Phys. Rev. B 35, 6716 (1987).
3. B. J. Sternlieb, G. M. Luke, Y. J. Uemura, T. M. Riseman, J. H. Brewer, P. M. Gehring, K. Yamada, Y. Hidaka, T. Murakami, T. R. Thurston, and R. J. Birgeneau, Phys. Rev. B 41, 8866 (1990).
4. E. Kruger, Phys. Rev. B 59, 13795 (1999).
5. E. Kruger, Phys. Rev. B 40, 11090 (1989).
6. E. Kruger, Phys. Rev. B 63, 144403 (2001).
7. E. Kruger, J. Supercond. 14 (4), 469 (2001).
8. E. Kruger, J. Supercond. 14 (4), 551 (2001).
9. E. Kruger, J. Supercond. 15 (2), 105 (2002).
10. N. F. Mott, Can. J. Phys. 34, 1356 (1956).
11. J. Hubbard, Proc. R. Soc. London, Ser. A 276, 238 (1963).
12. J. Bardeen, L. N. Cooper, and J. R. Schrieer, Phys. Rev. 108, 1175 (1957).
13. E. Kruger, phys. stat. sol. b 156, 345 (1989).
14. O. Jepsen, private communication.
15. E. Kruger, Phys. Rev. B 32, 7493 (1985).
16. C. Bradley and A. P. Cracknell, The Mathematical Theory of Symmetry in Solids (Claredon, Oxford, 1972).
17. E. Kruger, phys. stat. sol. b 52, 215 (1972).
18. E. Kruger, phys. stat. sol. b 52, 519 (1972).
19. E. Kruger, phys. stat. sol. b 61, 193 (1974).
20. E. Kruger, Phys. Rev. B 36, 2263 (1987).

TABLE I: Characters of the small (allowed) single-valued irreducible representations of the space group $I4/mmm = D_{4h}^{17}$ (139) of tetragonal La_2CuO_4 in the notation of Table 5.8 in the textbook of Bradley and Cracknell [16].

(000) and Z $(\frac{1}{2}\frac{1}{2}\frac{1}{2})$

		E	C_{2z}	C_{4z} / C_{4z}^{+}	C_{2y} / C_{2x}	C_{2b} / C_{2a}	I	z	S_{4z}^{+} / S_{4z}	y / x	db / da
$^{+}_{1}$	Z_1^{+}	1	1	1	1	1	1	1	1	1	1
$^{+}_{2}$	Z_2^{+}	1	1	1	−1	−1	1	1	1	−1	−1
$^{+}_{3}$	Z_3^{+}	1	1	−1	1	−1	1	1	−1	1	−1
$^{+}_{4}$	Z_4^{+}	1	1	−1	−1	1	1	1	−1	−1	1
$^{+}_{5}$	Z_5^{+}	2	−2	0	0	0	2	−2	0	0	0
$_{1}$	Z_1	1	1	1	1	1	−1	−1	−1	−1	−1
$_{2}$	Z_2	1	1	1	−1	−1	−1	−1	−1	1	1
$_{3}$	Z_3	1	1	−1	1	−1	−1	−1	1	−1	1
$_{4}$	Z_4	1	1	−1	−1	1	−1	−1	1	1	−1
$_{5}$	Z_5	2	−2	0	0	0	−2	2	0	0	0

N $(0\frac{1}{2}0)$

	E	C_{2y}	I	y
N_1^{+}	1	1	1	1
N_1	1	1	−1	−1
N_2^{+}	1	−1	1	−1
N_2	1	−1	−1	1

X $(00\frac{1}{2})$

	E	C_{2z}	C_{2a}	C_{2b}	I	z	da	db
X_1^{+}	1	1	1	1	1	1	1	1
X_2^{+}	1	−1	1	−1	1	−1	1	−1
X_3^{+}	1	1	−1	−1	1	1	−1	−1
X_4^{+}	1	−1	−1	1	1	−1	−1	1
X_1	1	1	1	1	−1	−1	−1	−1
X_2	1	−1	1	−1	−1	1	−1	1
X_3	1	1	−1	−1	−1	−1	1	1
X_4	1	−1	−1	1	−1	1	1	−1

P $(\frac{1}{4}\frac{1}{4}\frac{1}{4})$

	E	C_{2z}	S_{4z} / S_{4z}^{+}	C_{2y} / C_{2x}	da / db
P_1	1	1	1	1	1
P_2	1	1	1	−1	−1
P_3	1	1	−1	1	−1
P_4	1	1	−1	−1	1
P_5	2	−2	0	0	0

TABLE II: Characters of the small (allowed) single-valued irreducible representations of the space group $H = Cmca = D_{2h}^{18}$ (64) of the orthorhombic phase of La_2CuO_4 in the notation of Table 5.8 in the textbook of Bradley and Cracknell [16]. K stands for the operator of time-inversion. The first two elements in the first row define two magnetic groups $M_1 = H + KH$ and $M_2 = H + \{K|\frac{1}{2}\frac{1}{2}\frac{1}{2}\}H$. The second and third column of the table specify whether the corepresentations of M_1 and M_2, respectively, derived from the given representations R_i of H follow case (a), case (b), or case (c) when they are given by Eqs. (7.3.45–47) of Ref. [16]. In case (a), there is no change in the degeneracy of R_i, and in case (c) the degeneracy becomes doubled.

(000) and Y $(\bar{\frac{1}{2}}\frac{1}{2}0)$

		K	$\{K\|\frac{1}{2}\frac{1}{2}\frac{1}{2}\}$	$\{E\|000\}$	$\{C_{2a}\|\frac{1}{2}\frac{1}{2}\frac{1}{2}\}$	$\{C_{2z}\|\frac{1}{2}\frac{1}{2}\frac{1}{2}\}$	$\{C_{2b}\|000\}$	$\{I\|000\}$	$\{\sigma_{da}\|\frac{1}{2}\frac{1}{2}\frac{1}{2}\}$	$\{\sigma_z\|\frac{1}{2}\frac{1}{2}\frac{1}{2}\}$	$\{\sigma_{db}\|000\}$
$^+_1$	Y_1^+	(a)	(a)	1	1	1	1	1	1	1	1
$^+_2$	Y_2^+	(a)	(a)	1	−1	1	−1	1	−1	1	−1
$^+_3$	Y_3^+	(a)	(a)	1	1	−1	−1	1	1	−1	−1
$^+_4$	Y_4^+	(a)	(a)	1	−1	−1	1	1	−1	−1	1
$_1$	Y_1	(a)	(a)	1	1	1	1	−1	−1	−1	−1
$_2$	Y_2	(a)	(a)	1	−1	1	−1	−1	1	−1	1
$_3$	Y_3	(a)	(a)	1	1	−1	−1	−1	−1	1	1
$_4$	Y_4	(a)	(a)	1	−1	−1	1	−1	1	1	−1

Z $(00\frac{1}{2})$ and T $(\bar{\frac{1}{2}}\frac{1}{2}\frac{1}{2})$

	K	$\{K\|\frac{1}{2}\frac{1}{2}\frac{1}{2}\}$	$\{E\|000\}$	$\{E\|001\}$	$\{C_{2a}\|\frac{1}{2}\frac{1}{2}\frac{1}{2}\}$	$\{I\|000\}$	$\{\sigma_{da}\|\frac{1}{2}\frac{1}{2}\frac{1}{2}\}$	$\{\sigma_{db}\|000\}$	$\{\sigma_{db}\|001\}$	$\{\sigma_z\|\frac{1}{2}\frac{1}{2}\frac{1}{2}\}$	$\{C_{2b}\|000\}$	$\{C_{2z}\|\frac{1}{2}\frac{1}{2}\frac{1}{2}\}$
					$\{C_{2a}\|\frac{1}{2}\frac{1}{2}\frac{3}{2}\}$	$\{I\|001\}$	$\{\sigma_{da}\|\frac{1}{2}\frac{1}{2}\frac{3}{2}\}$			$\{\sigma_z\|\frac{1}{2}\frac{1}{2}\frac{3}{2}\}$	$\{C_{2b}\|001\}$	$\{C_{2z}\|\frac{1}{2}\frac{1}{2}\frac{3}{2}\}$
Z_1	(a)	(a)	2	−2	0	0	0	2	−2	0	0	0
Z_2	(a)	(a)	2	−2	0	0	0	−2	2	0	0	0

S $(0\frac{1}{2}0)$

	K	$\{K\|\frac{1}{2}\frac{1}{2}\frac{1}{2}\}$	$\{E\|000\}$	$\{E\|010\}$	$\{\sigma_{da}\|\frac{1}{2}\frac{1}{2}\frac{1}{2}\}$	$\{I\|000\}$	$\{C_{2a}\|\frac{1}{2}\frac{1}{2}\frac{1}{2}\}$
					$\{\sigma_{da}\|\frac{1}{2}\frac{3}{2}\frac{1}{2}\}$	$\{I\|010\}$	$\{C_{2a}\|\frac{1}{2}\frac{3}{2}\frac{1}{2}\}$
S_1	(a)	(a)	2	−2	0	0	0

R $(0\frac{1}{2}\frac{1}{2})$

	K	$\{K\|\frac{1}{2}\frac{1}{2}\frac{1}{2}\}$	$\{E\|000\}$	$\{\sigma_{da}\|\frac{1}{2}\frac{1}{2}\frac{1}{2}\}$	$\{E\|001\}$	$\{\sigma_{da}\|\frac{1}{2}\frac{1}{2}\frac{3}{2}\}$	$\{I\|000\}$	$\{C_{2a}\|\frac{1}{2}\frac{1}{2}\frac{1}{2}\}$	$\{I\|001\}$	$\{C_{2a}\|\frac{1}{2}\frac{1}{2}\frac{3}{2}\}$
R_1^+	(c)	(a)	1	i	−1	−i	1	i	−1	−i
R_2^+	(c)	(a)	1	−i	−1	i	1	−i	−1	i
R_1	(c)	(a)	1	i	−1	−i	−1	−i	1	i
R_2	(c)	(a)	1	−i	−1	i	−1	i	1	−i

TABLE III: Characters of the small (allowed) single-valued irreducible representations of the space group $H = Pccn = D_{2h}^{10}$ (56) of the antiferromagnetic structure of La_2CuO_4 in the notation of Table 5.8 in the textbook of Bradley and Cracknell [16]. K stands for the operator of time-inversion. The first three elements in the first row define three magnetic groups $M_1 = H + KH$; $M_2 = H + \{K|\frac{1}{2}\frac{1}{2}0\}H$; and $M_3 = H + \{K|0\frac{1}{2}\frac{1}{2}\}H$. The second, third, and fourth column of the table specify whether the corepresentations of M_1, M_2, and M_3, respectively, derived from the given representations R_i of H follow case (a), case (b), or case (c) when they are given by Eqs. (7.3.45-47) of Ref. [16]. In case (a), there is no change in the degeneracy of R_i, and in case (c) the degeneracy becomes doubled.

(000)

	K	$\{K\|\frac{1}{2}\frac{1}{2}0\}$	$\{K\|0\frac{1}{2}\frac{1}{2}\}$	$\{E\|000\}$	$\{C_{2z}\|\frac{1}{2}\frac{1}{2}0\}$	$\{C_{2b}\|0\frac{1}{2}\frac{1}{2}\}$	$\{C_{2a}\|\frac{1}{2}0\frac{1}{2}\}$	$\{I\|000\}$	$\{\sigma_z\|\frac{1}{2}\frac{1}{2}0\}$	$\{\sigma_{db}\|0\frac{1}{2}\frac{1}{2}\}$	$\{\sigma_{da}\|\frac{1}{2}0\frac{1}{2}\}$
$^+_1$	(a)	(a)	(a)	1	1	1	1	1	1	1	1
$^+_2$	(a)	(a)	(a)	1	−1	1	−1	1	−1	1	−1
$^+_3$	(a)	(a)	(a)	1	1	−1	−1	1	1	−1	−1
$^+_4$	(a)	(a)	(a)	1	−1	−1	1	1	−1	−1	1
$_1$	(a)	(a)	(a)	1	1	1	1	−1	−1	−1	−1
$_2$	(a)	(a)	(a)	1	−1	1	−1	−1	1	−1	1
$_3$	(a)	(a)	(a)	1	1	−1	−1	−1	−1	1	1
$_4$	(a)	(a)	(a)	1	−1	−1	1	−1	1	1	−1

$Y\ (\frac{1}{2}\bar{1}00)$

	K	$\{K\|\frac{1}{2}\frac{1}{2}0\}$	$\{K\|0\frac{1}{2}\frac{1}{2}\}$	$\{E\|000\}$	$\{E\|100\}$	$\{\sigma_z\|\frac{3}{2}\frac{1}{2}0\}$	$\{I\|000\}$	$\{\sigma_z\|\frac{1}{2}\frac{1}{2}0\}$	$\{I\|100\}$
Y_1	(a)	(a)	(a)	2	−2	0	0		
Y_2	(a)	(a)	(a)	2	−2	0	0		

$Y\ (\frac{1}{2}\bar{1}00)$ (continued)

	$\{C_{2z}\|\frac{1}{2}\frac{1}{2}0\}$	$\{C_{2z}\|\frac{3}{2}\frac{1}{2}0\}$	$\{\sigma_{da}\|\frac{1}{2}\frac{1}{2}\frac{1}{2}\}$	$\{\sigma_{da}\|1\frac{1}{2}\frac{1}{2}\}$	$\{C_{2b}\|\frac{3}{2}0\frac{1}{2}\}$	$\{C_{2a}\|\frac{1}{2}\frac{1}{2}\frac{1}{2}\}$	$\{\sigma_{db}\|\frac{1}{2}0\frac{1}{2}\}$	$\{C_{2b}\|\frac{1}{2}0\frac{1}{2}\}$	$\{C_{2a}\|1\frac{1}{2}\frac{1}{2}\}$	$\{\sigma_{db}\|\frac{3}{2}0\frac{1}{2}\}$
Y_1	0		2	−2	0		0		0	
Y_2	0		−2	2	0		0		0	

$X\ (0\frac{1}{2}0)$

	K	$\{K\|\frac{1}{2}\frac{1}{2}0\}$	$\{K\|0\frac{1}{2}\frac{1}{2}\}$	$\{E\|000\}$	$\{E\|010\}$	$\{\sigma_z\|\frac{1}{2}\frac{3}{2}0\}$	$\{I\|010\}$	$\{\sigma_z\|\frac{1}{2}\frac{1}{2}0\}$	$\{I\|000\}$
X_1	(a)	(a)	(a)	2	−2	0	0		
X_2	(a)	(a)	(a)	2	−2	0	0		

$X\ (0\frac{1}{2}0)$ (continued)

	$\{C_{2z}\|\frac{1}{2}\frac{1}{2}0\}$	$\{C_{2z}\|\frac{1}{2}\frac{3}{2}0\}$	$\{\sigma_{db}\|\frac{1}{2}0\frac{1}{2}\}$	$\{\sigma_{db}\|\frac{1}{2}1\frac{1}{2}\}$	$\{C_{2a}\|\frac{3}{2}\frac{1}{2}\frac{1}{2}\}$	$\{C_{2a}\|\frac{1}{2}\frac{1}{2}\frac{1}{2}\}$	$\{C_{2b}\|\frac{1}{2}1\frac{1}{2}\}$	$\{C_{2b}\|\frac{1}{2}0\frac{1}{2}\}$	$\{\sigma_{da}\|\frac{3}{2}\frac{1}{2}\frac{1}{2}\}$	$\{\sigma_{da}\|\frac{1}{2}\frac{1}{2}\frac{1}{2}\}$
X_1	0		2	−2	0		0		0	
X_2	0		−2	2	0		0		0	

$Z\ (00\frac{1}{2})$

	K	$\{K\|\frac{1}{2}\frac{1}{2}0\}$	$\{K\|0\frac{1}{2}\frac{1}{2}\}$	$\{E\|000\}$	$\{E\|001\}$	$\{\sigma_{da}\|\frac{1}{2}\frac{3}{2}\frac{1}{2}\}$	$\{I\|001\}$	$\{\sigma_{da}\|\frac{1}{2}\frac{1}{2}\frac{1}{2}\}$	$\{I\|000\}$
Z_1	(a)	(a)	(a)	2	−2	0	0		
Z_2	(a)	(a)	(a)	2	−2	0	0		

$Z\ (00\frac{1}{2})$ (continued)

	$\{C_{2a}\|\frac{1}{2}\frac{1}{2}\frac{1}{2}\}$	$\{C_{2a}\|\frac{1}{2}\frac{3}{2}\frac{1}{2}\}$	$\{C_{2z}\|\frac{1}{2}\frac{1}{2}0\}$	$\{C_{2z}\|\frac{1}{2}\frac{1}{2}1\}$	$\{\sigma_{db}\|\frac{1}{2}0\frac{1}{2}\}$	$\{\sigma_{db}\|\frac{1}{2}0\frac{3}{2}\}$	$\{\sigma_z\|\frac{1}{2}\frac{1}{2}0\}$	$\{\sigma_z\|\frac{1}{2}\frac{1}{2}1\}$	$\{C_{2b}\|\frac{1}{2}0\frac{1}{2}\}$	$\{C_{2b}\|\frac{1}{2}0\frac{3}{2}\}$
Z_1	0		2	−2	0		0		0	
Z_2	0		−2	2	0		0		0	

TABLE III: continued

$U(0\frac{1}{2}\frac{1}{2})$

	K	$\{K\|\frac{1}{2}\frac{1}{2}0\}$	$\{K\|\frac{1}{2}0\frac{1}{2}\}$	$\{E\|000\}$	$\{d_a\|\frac{1}{2}\frac{1}{2}\frac{3}{2}\}$	$\{E\|001\}$	$\{d_a\|\frac{1}{2}\frac{1}{2}\frac{1}{2}\}$
U_1	(c)	(a)	(c)	2	$2i$	-2	$-2i$
U_2	(c)	(a)	(c)	2	$-2i$	-2	$2i$

$U(0\frac{1}{2}\frac{1}{2})$ (continued)

	$\{C_{2z}\|\frac{1}{2}\frac{1}{2}0\}$	$\{d_b\|\frac{1}{2}0\frac{3}{2}\}$	$\{I\|001\}$	$\{C_{2a}\|\frac{1}{2}\frac{1}{2}\frac{1}{2}\}$	$\{\sigma_z\|\frac{1}{2}\frac{1}{2}0\}$	$\{C_{2b}\|\frac{1}{2}0\frac{3}{2}\}$
	$\{C_{2z}\|\frac{1}{2}\frac{1}{2}1\}$	$\{d_b\|\frac{1}{2}0\frac{1}{2}\}$	$\{I\|000\}$	$\{C_{2a}\|\frac{1}{2}\frac{1}{2}\frac{3}{2}\}$	$\{\sigma_z\|\frac{1}{2}\frac{1}{2}1\}$	$\{C_{2b}\|\frac{1}{2}0\frac{1}{2}\}$
U_1	0	0	0	0	0	0
U_2	0	0	0	0	0	0

$T(\bar{\frac{1}{2}}0\frac{1}{2})$

	K	$\{K\|\frac{1}{2}\frac{1}{2}0\}$	$\{K\|\frac{1}{2}0\frac{1}{2}\}$	$\{E\|000\}$	$\{d_b\|\frac{1}{2}0\frac{1}{2}\}$	$\{E\|001\}$	$\{d_b\|\frac{1}{2}0\frac{3}{2}\}$
T_1	(c)	(a)	(a)	2	$2i$	-2	$-2i$
T_2	(c)	(a)	(a)	2	$-2i$	-2	$2i$

$T(\bar{\frac{1}{2}}0\frac{1}{2})$ (continued)

	$\{C_{2z}\|\frac{1}{2}\frac{1}{2}1\}$	$\{d_a\|\frac{1}{2}\frac{1}{2}\frac{3}{2}\}$	$\{I\|000\}$	$\{C_{2b}\|\frac{1}{2}0\frac{1}{2}\}$	$\{\sigma_z\|\frac{1}{2}\frac{1}{2}0\}$	$\{C_{2a}\|\frac{1}{2}\frac{1}{2}\frac{1}{2}\}$
	$\{C_{2z}\|\frac{1}{2}\frac{1}{2}0\}$	$\{d_a\|\frac{1}{2}\frac{1}{2}\frac{1}{2}\}$	$\{I\|001\}$	$\{C_{2b}\|\frac{1}{2}0\frac{3}{2}\}$	$\{\sigma_z\|\frac{1}{2}\frac{1}{2}1\}$	$\{C_{2a}\|\frac{1}{2}\frac{1}{2}\frac{3}{2}\}$
T_1	0	0	0	0	0	0
T_2	0	0	0	0	0	0

$S(\bar{\frac{1}{2}}\frac{1}{2}0)$

	K	$\{K\|\frac{1}{2}\frac{1}{2}0\}$	$\{K\|\frac{1}{2}0\frac{1}{2}\}$	$\{E\|000\}$	$\{E\|010\}$	$\{C_{2b}\|\frac{1}{2}1\frac{1}{2}\}\{I\|000\}$	$\{C_{2b}\|\frac{1}{2}0\frac{1}{2}\}\{I\|010\}$
S_1	(a)	(a)	(c)	2	-2	0	0
S_2	(a)	(a)	(c)	2	-2	0	0

$S(\bar{\frac{1}{2}}\frac{1}{2}0)$ (continued)

	$\{d_b\|\frac{1}{2}0\frac{1}{2}\}$			$\{C_{2a}\|\frac{1}{2}\frac{1}{2}\frac{1}{2}\}$	$\{\sigma_z\|\frac{1}{2}\frac{3}{2}0\}$	$\{d_a\|\frac{3}{2}\frac{1}{2}\}$
	$\{d_b\|\frac{1}{2}1\frac{1}{2}\}$	$\{C_{2z}\|\frac{1}{2}\frac{3}{2}0\}$	$\{C_{2z}\|\frac{1}{2}\frac{1}{2}0\}$	$\{C_{2a}\|\frac{3}{2}\frac{1}{2}\}$	$\{\sigma_z\|\frac{1}{2}\frac{1}{2}0\}$	$\{d_a\|\frac{1}{2}\frac{1}{2}\}$
S_1	0	2	-2	0	0	0
S_2	0	-2	2	0	0	0

$R(\bar{\frac{1}{2}}\frac{1}{2}\frac{1}{2})$

	K	$\{K\|\frac{1}{2}\frac{1}{2}0\}$	$\{K\|\frac{1}{2}0\frac{1}{2}\}$	$\{E\|000\}$	$\{C_{2a}\|\frac{1}{2}\frac{1}{2}\frac{1}{2}\}$	$\{E\|001\}$	$\{C_{2a}\|\frac{1}{2}\frac{1}{2}\frac{3}{2}\}$	$\{C_{2z}\|\frac{1}{2}\frac{1}{2}1\}$	$\{C_{2b}\|\frac{1}{2}0\frac{3}{2}\}$	$\{C_{2z}\|\frac{1}{2}\frac{1}{2}0\}$
R_1	(c)	(a)	(c)	1	i	-1	$-i$	1	i	-1
R_2	(c)	(a)	(c)	1	$-i$	-1	i	1	$-i$	-1
R_3	(c)	(a)	(c)	1	i	-1	$-i$	-1	$-i$	1
R_4	(c)	(a)	(c)	1	$-i$	-1	i	-1	i	1
R_1^+	(c)	(a)	(c)	1	i	-1	$-i$	1	i	-1
R_2^+	(c)	(a)	(c)	1	$-i$	-1	i	1	$-i$	-1
R_3^+	(c)	(a)	(c)	1	i	-1	$-i$	-1	$-i$	1
R_4^+	(c)	(a)	(c)	1	$-i$	-1	i	-1	i	1

$R(\bar{\frac{1}{2}}\frac{1}{2}\frac{1}{2})$ (continued)

	$\{C_{2b}\|\frac{1}{2}0\frac{1}{2}\}$	$\{I\|001\}$	$\{d_a\|\frac{1}{2}\frac{1}{2}\frac{3}{2}\}$	$\{I\|000\}$	$\{d_a\|\frac{1}{2}\frac{1}{2}\frac{1}{2}\}$	$\{\sigma_z\|\frac{1}{2}\frac{1}{2}0\}$	$\{d_b\|\frac{1}{2}0\frac{1}{2}\}$	$\{\sigma_z\|\frac{1}{2}\frac{1}{2}1\}$	$\{d_b\|\frac{1}{2}0\frac{3}{2}\}$
R_1	$-i$	1	i	-1	$-i$	1	i	-1	$-i$
R_2	i	1	$-i$	-1	i	1	$-i$	-1	i
R_3	i	1	i	-1	$-i$	-1	$-i$	1	i
R_4	$-i$	1	$-i$	-1	i	-1	i	1	$-i$
R_1^+	$-i$	-1	$-i$	1	i	-1	$-i$	1	i
R_2^+	i	-1	i	1	$-i$	-1	i	1	$-i$
R_3^+	i	-1	$-i$	1	i	1	i	-1	$-i$
R_4^+	$-i$	-1	i	1	$-i$	1	$-i$	-1	i

TABLE IV: Characters of the small (allowed) double-valued irreducible representations of the space group I4/mmm of tetragonal La_2CuO_4 in the notation of Table 5.8 in the textbook of Bradley and Cracknell [16].

(000) and Z $(\frac{1}{2}\frac{1}{2}\frac{1}{2})$

	E	$\bar{E}$	C_{2z}	C_{4z}	$\bar{C}^{+}_{4z}$	$\bar{C}_{2x}$	$\bar{C}_{2y}$	$\bar{C}_{2b}$	C_{2a}	C_{2b}	I	$\bar{I}$	z	$\bar{z}$	S^{+}_{4z}	S_{4z}	$\bar{S}_{4z}$	$\bar{S}^{+}_{4z}$	x	y	$\bar{x}$	$\bar{y}$	db	da	$\bar{db}$	$\bar{da}$
Γ^{+}_{6} Z^{+}_{6}	2	−2	0	$\sqrt{2}$	$-\sqrt{2}$	0	0	0	0	2	−2	0			$\sqrt{2}$	$-\sqrt{2}$	0	0								
Γ^{+}_{7} Z^{+}_{7}	2	−2	0	$-\sqrt{2}$	$\sqrt{2}$	0	0	0	0	2	−2	0			$-\sqrt{2}$	$\sqrt{2}$	0	0								
Γ_{6} Z_{6}	2	−2	0	$\sqrt{2}$	$-\sqrt{2}$	0	0	0	0	−2	2	0			$-\sqrt{2}$	$\sqrt{2}$	0	0								
Γ_{7} Z_{7}	2	−2	0	$-\sqrt{2}$	$\sqrt{2}$	0	0	0	0	−2	2	0			$\sqrt{2}$	$-\sqrt{2}$	0	0								

N $(0\frac{1}{2}0)$

	E	C_{2y}	$\bar{E}$	$\bar{C}_{2y}$	I	y	$\bar{I}$	$\bar{y}$
N^{+}_{3}	1	i	−1	$-i$	1	i	−1	$-i$
N^{+}_{4}	1	$-i$	−1	i	1	$-i$	−1	i
N_{3}	1	i	−1	$-i$	−1	$-i$	1	i
N_{4}	1	$-i$	−1	i	−1	i	1	$-i$

X $(00\frac{1}{2})$

	E	$\bar{E}$	$\bar{C}_{2z}$	C_{2a}	$\bar{C}_{2b}$	I	$\bar{I}$	z	$\bar{z}$	da	db	$\bar{da}$	$\bar{db}$
X^{+}_{5}	2	−2	0	0	0	2	−2	0		0		0	
X_{5}	2	−2	0	0	0	−2	2	0		0		0	

P $(\frac{1}{4}\frac{1}{4}\frac{1}{4})$

	E	$\bar{E}$	$\bar{C}_{2z}$	S_{4z}	$\bar{S}^{+}_{4z}$	$\bar{C}_{2x}$	C_{2y}	$\bar{C}_{2y}$	C_{2x}	da	$\bar{db}$	$\bar{da}$	db
P_{6}	2	−2	0	$\sqrt{2}$	$-\sqrt{2}$	0				0			0
P_{7}	2	−2	0	$-\sqrt{2}$	$\sqrt{2}$	0				0			0

TABLE V: Characters of the small (allowed) double-valued irreducible representations of the space group Cmca of the orthorhombic phase of La_2CuO_4 in the notation of Table 5.8 in the textbook of Bradley and Cracknell [16].

(000) and Y $(\bar{\tfrac{1}{2}}\tfrac{1}{2}0)$

	$\{E\|000\}$	$\{\bar{E}\|000\}$	$\{C_{2a}\|\tfrac{1}{2}\tfrac{1}{2}\tfrac{1}{2}\}$	$\{C_{2z}\|\tfrac{1}{2}\tfrac{1}{2}\tfrac{1}{2}\}$	$\{C_{2b}\|000\}$	$\{I\|000\}$	$\{\bar{I}\|000\}$	$\{\sigma_{da}\|\tfrac{1}{2}\tfrac{1}{2}\tfrac{1}{2}\}$	$\{\sigma_{z}\|\tfrac{1}{2}\tfrac{1}{2}\tfrac{1}{2}\}$	$\{\sigma_{db}\|000\}$
${}^{+}_{5}$ Y_5^+	2	−2	0	0	0	2	−2	0	0	0
${}_{5}$ Y_5	2	−2	0	0	0	−2	2	0	0	0

Z $(00\tfrac{1}{2})$ and T $(\bar{\tfrac{1}{2}}\tfrac{1}{2}\tfrac{1}{2})$

	$\{E\|000\}$	$\{\bar{E}\|01\tfrac{1}{2}\}$	$\{\bar{E}\|00\tfrac{1}{2}\}$	$\{E\|01\tfrac{1}{2}\}$	$\{C_{2a}\|\tfrac{1}{2}\tfrac{1}{2}\tfrac{1}{2}\}$, $\{\bar{C}_{2a}\|\tfrac{1}{2}\tfrac{1}{2}\tfrac{1}{2}\}$, $\{\bar{C}_{2a}\|\tfrac{1}{2}\tfrac{1}{2}\tfrac{3}{2}\}$, $\{C_{2a}\|\tfrac{1}{2}\tfrac{1}{2}\tfrac{3}{2}\}$	$\{\bar{C}_{2b}\|01\tfrac{1}{2}\}$	$\{C_{2b}\|01\tfrac{1}{2}\}$, $\{C_{2a}\|\tfrac{1}{2}\tfrac{1}{2}\tfrac{1}{2}\}$, $\{\bar{C}_{2b}\|00\tfrac{1}{2}\}$
Z_3 T_3	2	2	−2	−2	0	2i	−2i
Z_4 T_4	2	2	−2	−2	0	−2i	2i

Z $(00\tfrac{1}{2})$ and T $(\bar{\tfrac{1}{2}}\tfrac{1}{2}\tfrac{1}{2})$ (continued)

	$\{C_{2z}\|\tfrac{1}{2}\tfrac{1}{2}\tfrac{1}{2}\}$, $\{C_{2z}\|\tfrac{1}{2}\tfrac{1}{2}\tfrac{3}{2}\}$, $\{\bar{C}_{2z}\|\tfrac{1}{2}\tfrac{1}{2}\tfrac{3}{2}\}$, $\{\bar{C}_{2z}\|\tfrac{1}{2}\tfrac{1}{2}\tfrac{1}{2}\}$	$\{I\|01\tfrac{1}{2}\}$	$\{\bar{I}\|00\tfrac{1}{2}\}$	$\{\sigma_{da}\|\tfrac{1}{2}\tfrac{1}{2}\tfrac{1}{2}\}$, $\{\sigma_{da}\|\tfrac{1}{2}\tfrac{1}{2}\tfrac{3}{2}\}$, $\{\sigma_{da}\|\tfrac{1}{2}\tfrac{1}{2}\tfrac{3}{2}\}$, $\{\sigma_{da}\|\tfrac{1}{2}\tfrac{1}{2}\tfrac{1}{2}\}$	$\{\sigma_{db}\|00\tfrac{1}{2}\}$	$\{\sigma_{db}\|01\tfrac{1}{2}\}$	$\{\sigma_{z}\|\tfrac{1}{2}\tfrac{1}{2}\tfrac{1}{2}\}$, $\{\sigma_{z}\|\tfrac{1}{2}\tfrac{1}{2}\tfrac{3}{2}\}$, $\{\sigma_{z}\|\tfrac{1}{2}\tfrac{1}{2}\tfrac{3}{2}\}$, $\{\sigma_{z}\|\tfrac{1}{2}\tfrac{1}{2}\tfrac{1}{2}\}$
Z_3 T_3	0	0	0	0	0	0	0
Z_4 T_4	0	0	0	0	0	0	0

S $(0\tfrac{1}{2}0)$

	$\{E\|000\}$	$\{E\|010\}$	$\{\bar{E}\|010\}$	$\{\bar{E}\|000\}$	$\{I\|000\}$	$\{I\|010\}$, $\{\bar{I}\|000\}$	$\{\bar{I}\|010\}$	$\{\sigma_{da}\|\tfrac{1}{2}\tfrac{3}{2}\tfrac{1}{2}\}$, $\{\sigma_{da}\|\tfrac{1}{2}\tfrac{1}{2}\tfrac{1}{2}\}$, $\{\sigma_{da}\|\tfrac{1}{2}\tfrac{1}{2}\tfrac{1}{2}\}$, $\{\sigma_{da}\|\tfrac{1}{2}\tfrac{3}{2}\tfrac{1}{2}\}$	$\{C_{2a}\|\tfrac{1}{2}\tfrac{3}{2}\tfrac{1}{2}\}$, $\{C_{2a}\|\tfrac{1}{2}\tfrac{1}{2}\tfrac{1}{2}\}$, $\{C_{2a}\|\tfrac{1}{2}\tfrac{1}{2}\tfrac{1}{2}\}$	$\{\bar{C}_{2a}\|\tfrac{1}{2}\tfrac{1}{2}\tfrac{1}{2}\}$, $\{\bar{C}_{2a}\|\tfrac{1}{2}\tfrac{3}{2}\tfrac{1}{2}\}$
S_2	2	−2	2	−2	0	0	0	0	0	0

R $(0\tfrac{1}{2}\tfrac{1}{2})$

	$\{E\|000\}$	$\{\sigma_{da}\|\tfrac{1}{2}\tfrac{1}{2}\tfrac{1}{2}\}$	$\{\bar{E}\|01\tfrac{1}{2}\}$	$\{\sigma_{da}\|\tfrac{1}{2}\tfrac{1}{2}\tfrac{3}{2}\}$	$\{I\|000\}$	$\{C_{2a}\|\tfrac{1}{2}\tfrac{1}{2}\tfrac{1}{2}\}$	$\{\bar{I}\|01\tfrac{1}{2}\}$	$\{\bar{C}_{2a}\|\tfrac{1}{2}\tfrac{1}{2}\tfrac{3}{2}\}$
R_3^+	1	1	1	1	1	1	1	1
R_4^+	1	−1	1	−1	1	−1	1	−1
R_3	1	1	1	1	−1	−1	−1	−1
R_4	1	−1	1	−1	−1	1	−1	1

TABLE VI: Compatibility relations between the single-valued representations of the space group I4/mmm of tetragonal La_2CuO_4 and the single-valued representations of the space group Cmca of the orthorhombic phase of La_2CuO_4. For the notations see Tables I and II. The upper row lists small representations at the points of symmetry in the Brillouin zone of I4/mmm and the lower row lists small representations at the related points of symmetry in the Brillouin zone of Cmca (cf. Fig. 4). The small representations in the same column are compatible in the following sense: Bloch functions which are basis functions of a small representation R_i in the upper row also form basis functions of the small representation standing below R_i.

1^+	2^+	3^+	4^+		5^+		1	2	3	4		5
1^+	2^+	2^+	1^+	3^+	$+$	4^+	1	2	2	1	3	$+$ 4

X_1^+	X_2^+	X_3^+	X_4^+	X_1	X_2	X_3	X_4
4^+	2^+	3^+	1^+	4	2	3	1

Y

Z_1^+	Z_2^+	Z_3^+	Z_4^+		Z_5^+		Z_1	Z_2	Z_3	Z_4		Z_5
Y_1^+	Y_2^+	Y_2^+	Y_1^+	Y_3^+	$+$	Y_4^+	Y_1	Y_2	Y_2	Y_1	Y_3	$+$ Y_4

Y

X_1^+	X_2^+	X_3^+	X_4^+	X_1	X_2	X_3	X_4
Y_4^+	Y_1^+	Y_3^+	Y_2^+	Y_4	Y_1	Y_3	Y_2

R

N_1^+	N_1	N_2^+	N_2
$R_1^+ + R_2^+$	$R_1 + R_2$	$R_1^+ + R_2^+$	$R_1 + R_2$

T

U_1	U_3	U_2	U_4
T_1	T_2	T_2	T_1

Z

1	3	2	4
Z_1	Z_2	Z_2	Z_1

S

E_1^0	E_2^0
S_1	S_1

TABLE VII: Compatibility relations between the single-valued representations of the space group I4/mmm of tetragonal La_2CuO_4 and the single-valued representations of the space group P4/mnc of antiferromagnetic chromium. For the notations see Table I and Table II of Ref. [15]. The upper row lists small representations at the points of symmetry in the Brillouin zone of I4/mmm and the lower row lists small representations at the related points of symmetry in the Brillouin zone of P4/mnc. The small representations in the same column are compatible in the following sense: Bloch functions which are basis functions of a small representation R_i in the upper row also form basis functions of the small representation standing below R_i.

1^+	2^+	3^+	4^+	5^+	1	2	3	4	5
1^+	2^+	3^+	4^+	5^+	1	2	3	4	5

Z_1^+	Z_2^+	Z_3^+	Z_4^+	Z_5^+	Z_1	Z_2	Z_3	Z_4	Z_5
2^+	1^+	4^+	3^+	5^+	2	1	4	3	5

M

X_1^+	X_2^+	X_3^+	X_4^+	X_1	X_2	X_3	X_4
M_{20}	$M_{17} + M_{18}$	M_{20}	$M_{15} + M_{16}$	M_{10}	$M_5 + M_6$	M_{10}	$M_7 + M_8$

A

P_1	P_2	P_3	P_4	P_5
A_{11}	A_{11}	A_{10}	A_{10}	$A_{12} + A_{13}$

X

1	3	2	4
X_5	X_{10}	X_5	X_{10}

Z

1	2	3	4	5
Z_{10}	Z_{10}	Z_{11}	Z_{11}	$Z_{12} + Z_{13}$

R

N_1^+	N_1	N_2^+	N_2
R_5	R_{10}	R_5	R_{10}

TABLE VIII: Compatibility relations between the single-valued representations of the space group Cmca of the orthorhombic phase of La_2CuO_4 and the single-valued representations of the space group Pccn of the antiferromagnetic structure of La_2CuO_4. For the notations see Tables II and III. The upper row lists small representations at the points of symmetry in the Brillouin zone of Cmca and the lower row lists small representations at the related points of symmetry in the Brillouin zone of Pccn (cf. Fig. 4). The small representations in the same column are compatible in the following sense: Bloch functions which are basis functions of a small representation R_i in the upper row also form basis functions of the small representation standing below R_i.

1^+	2^+	3^+	4^+	1	2	3	4
1^+	3^+	4^+	2^+	1	3	4	2

Y_1^+	Y_2^+	Y_3^+	Y_4^+	Y_1	Y_2	Y_3	Y_4
3^+	1^+	2^+	4^+	3	1	2	4

X	X	T	S	R			
Z_1	Z_2	T_1	T_2	S_1	A_1	R_1^+	R_2^+	R_1	R_2
X_1	X_2	X_2	X_1	$T_1 + T_2$	$S_1 + S_2$	$R_1^+ + R_3^+$	$R_2^+ + R_4^+$	$R_2 + R_4$	$R_1 + R_3$

Y				U				Z			
1	3	2	4	B_1	B_2	B_3	B_4	1	3	2	4
Y_1	Y_2	Y_1	Y_2	U_1	U_2	U_2	U_1	Z_1	Z_1	Z_2	Z_2

TABLE IX: Compatibility relations between the single-valued (upper row) and double-valued (lower row) representations of the space group I4/mmm of tetragonal La_2CuO_4. For the notations see Tables I and IV. The small representations in the same column are compatible in the following sense: spin-dependent Bloch functions which are basis functions of the small representation $R_i \quad D_{1/2}$ (with R_i standing in the upper row) also form basis functions of the double-valued small representation standing below R_i. $D_{1/2}$ denotes the two-dimensional double-valued representation of the three-dimensional rotation group O(3) (given, e.g., in Table 6.1 of Ref. [16]).

1^+	2^+	3^+	4^+		5^+		1	2	3	4		5	
6^+	6^+	7^+	7^+	6^+	+	7^+	6	6	7	7	6	+	7

Z													
Z_1^+	Z_2^+	Z_3^+	Z_4^+		Z_5^+		Z_1	Z_2	Z_3	Z_4		Z_5	
Z_6^+	Z_6^+	Z_7^+	Z_7^+	Z_6^+	+	Z_7^+	Z_6	Z_6	Z_7	Z_7	Z_6	+	Z_7

N				X				P					
N_1^+		N_1		N_2^+		N_2		X_1^+	X_2^+	X_3^+	X_4^+	X_1	X_2	X_3	X_4	P_1	P_2	P_3	P_4		P_5
N_3^+	+	N_4^+	N_3 + N_4	N_3^+	+	N_4^+	N_3 + N_4	X_5^+	X_5^+	X_5^+	X_5^+	X_5	X_5	X_5	X_5	P_6	P_6	P_7	P_7	P_6 +	P_7

TABLE X: Compatibility relations between the single-valued (upper row) and double-valued (lower row) representations of the space group Cmca of the orthorhombic phase of La_2CuO_4. For the notations see Tables II and V. The small representations in the same column are compatible in the following sense: spin-dependent Bloch functions which are basis functions of the small representation $R_i \quad D_{1/2}$ (with R_i standing in the upper row) also form basis functions of the double-valued representation standing below R_i. $D_{1/2}$ denotes the two-dimensional double-valued representation of the three-dimensional rotation group O(3) (given, e.g., in Table 6.1 of Ref. [16]).

1^+	2^+	3^+	4^+	1	2	3	4
5^+	5^+	5^+	5^+	5	5	5	5

Y							
Y_1^+	Y_2^+	Y_3^+	Y_4^+	Y_1	Y_2	Y_3	Y_4
Y_5^+	Y_5^+	Y_5^+	Y_5^+	Y_5	Y_5	Y_5	Y_5

Z		T		S	R			
Z_1	Z_2	T_1	T_2	S_1	R_1^+	R_2^+	R_1	R_2
$Z_3 + Z_4$	$Z_3 + Z_4$	$T_3 + T_4$	$T_3 + T_4$	$2S_2$	$R_3^+ + R_4^+$	$R_3^+ + R_4^+$	$R_3 + R_4$	$R_3 + R_4$

TABLE XI: Single-valued small representations (in the notation given in Table I) of all the single bands in the space group $I4/mmm$ of tetragonal La_2CuO_4 with symmetry-adapted and optimally localizable Wannier functions centered at the Cu atoms.

Band 1	Γ_1^+	Z_1^+	N_1^+	X_1^+	P_1
Band 2	Γ_2^+	Z_2^+	N_2^+	X_3^+	P_2
Band 3	Γ_3^+	Z_3^+	N_1^+	X_3^+	P_3
Band 4	Γ_4^+	Z_4^+	N_2^+	X_1^+	P_4
Band 5	Γ_1	Z_1	N_1	X_1	P_3
Band 6	Γ_2	Z_2	N_2	X_3	P_4
Band 7	Γ_3	Z_3	N_1	X_3	P_1
Band 8	Γ_4	Z_4	N_2	X_1	P_2

TABLE XII: (Double-valued) small representations (in the notation given in Table IV) of all the superconducting bands in the space group $I4/mmm$ of tetragonal La_2CuO_4 with symmetry-adapted and optimally localizable spin-dependent Wannier functions centered at the Cu atoms.

Band 1	$\bar{\Gamma}_6^+$	Z_6^+	$N_3^+ + N_4^+$	X_5^+	P_6
Band 2	$\bar{\Gamma}_7^+$	Z_7^+	$N_3^+ + N_4^+$	X_5^+	P_7
Band 3	$\bar{\Gamma}_6$	Z_6	$N_3 + N_4$	X_5	P_7
Band 4	$\bar{\Gamma}_7$	Z_7	$N_3 + N_4$	X_5	P_6

TABLE XIII: (Double-valued) small representations (in the notation given in Table V) of all the superconducting bands in the space group $Cmca$ of the orthorhombic phase of La_2CuO_4 with symmetry-adapted and optimally localizable spin-dependent Wannier functions centered at the Cu atoms.

Band 1	$2\bar{\Gamma}_5^+$	$2Y_5^+$	$Z_3 + Z_4$	$T_3 + T_4$	$2S_2$ $2R_3^+ + 2R_4^+$
Band 2	$2\bar{\Gamma}_5$	$2Y_5$	$Z_3 + Z_4$	$T_3 + T_4$	$2S_2$ $2R_3 + 2R_4$

TABLE XIV: (Single-valued) small representations (in the notation given in Table II) of all the neutral bands in the space group $Cmca$ of the orthorhombic phase of La_2CuO_4 with symmetry-adapted and optimally localizable Wannier functions centered at the Cu atoms. The Wannier functions may be constructed so that either they are symmetry-adapted to the magnetic group $M_1 = Cmca + \{K \mid \frac{1}{2}\frac{1}{2}\frac{1}{2}\}Cmca$ or to the grey magnetic group $M_2 = Cmca + K \quad Cmca$ because Eq. (B16) is satisfied in both cases. However, an antiferromagnetic structure with the magnetic group M_1 is unstable, see Appendix A. Hence, the listed bands are neutral bands with Wannier functions adapted to M_2.

Band 1	$\Gamma_1^+ + \Gamma_4^+$	$Y_1^+ + Y_4^+$	Z_1	T_1	S_1 $R_1^+ + R_2^+$
Band 2	$\Gamma_2^+ + \Gamma_3^+$	$Y_2^+ + Y_3^+$	Z_2	T_2	S_1 $R_1^+ + R_2^+$
Band 3	$\Gamma_1 + \Gamma_4$	$Y_1 + Y_4$	Z_2	T_2	S_1 $R_1 + R_2$
Band 4	$\Gamma_2 + \Gamma_3$	$Y_2 + Y_3$	Z_1	T_1	S_1 $R_1 + R_2$

TABLE XV: (Single-valued) small representations (in the notation of Ref. [15]) of all the antiferromagnetic bands in the space group $P4/mnc = D_{4h}^6$ (128) of antiferromagnetic Cr with symmetry-adapted and optimally localizable Wannier functions centered at the Cu atoms. This table has already been published in Ref. [20].

Band 1	$\Gamma_1^+ + \Gamma_2^+$	X_5	M_{20}	A_{11}	Z_{10}	R_5
Band 2	$\Gamma_3^+ + \Gamma_4^+$	X_5	M_{20}	A_{10}	Z_{11}	R_5
Band 3	$\Gamma_1 + \Gamma_2$	X_{10}	M_{10}	A_{10}	Z_{10}	R_{10}
Band 4	$\Gamma_3 + \Gamma_4$	X_{10}	M_{10}	A_{11}	Z_{11}	R_{10}

TABLE XVI: (Single-valued) small representations (in the notation given in Table III) of all the antiferromagnetic bands in the space group Pccn of the (experimentally established) antiferromagnetic structure of La_2CuO_4 with symmetry-adapted and optimally localizable Wannier functions centered at the Cu atoms. An antiferromagnetic structure with the magnetic group $M = Pccn + \{K \mid \frac{1}{2}\frac{1}{2}0\}Pccn$ can be stable, see Appendix A.

Band 1	$^{+}_{1}$	+	$^{+}_{2}$	+	$^{+}_{3}$	+	$^{+}_{4}$	Y_1	+	Y_2	X_1	+	X_2	Z_1	+	Z_2	U_1	+	U_2	T_1	+	T_2	S_1	+	S_2	R^{+}_{1}	+	R^{+}_{2}	+	R^{+}_{3}	+	R^{+}_{4}
Band 2	$_{1}$	+	$_{2}$	+	$_{3}$	+	$_{4}$	Y_1	+	Y_2	X_1	+	X_2	Z_1	+	Z_2	U_1	+	U_2	T_1	+	T_2	S_1	+	S_2	R_1	+	R_2	+	R_3	+	R_4